Acoustic tweezers: patterning cells and microparticles using standing surface acoustic waves (SSAW)

Jinjie Shi,[a] Daniel Ahmed,[a] Xiaole Mao,[a,b] Sz-Chin Steven Lin,[a] Aitan Lewit[a] and Tony Jun Huang[*a,b]

[a] *Department of Engineering Science and Mechanics, The Pennsylvania State University, University Park, PA 16802, USA. Fax: 814-865-9974; Tel: 814-863-4209; E-mail: junhuang@psu.edu*
[b] *Department of Bioengineering, The Pennsylvania State University, University Park, PA 16802, USA.*

1. Device Fabrication

There were three major steps involved in the fabrication of the SSAW-based patterning device (Fig. S1): (1) the fabrication of a SAW substrate, (2) the fabrication of a polydimethylsiloxane (PDMS) microchannel, and (3) the bonding of the PDMS microchannel onto the SAW substrate. Figure S1 (a–d) shows the fabrication process of the SAW substrate. A layer of photoresist (SPR3012, MicroChem, Newton, MA) was spin-coated on a Y+128° X-propagation lithium niobate (LiNbO$_3$) wafer, patterned with a UV light source, and developed in a photoresist developer (MF CD-26, Microposit). A double metal layer (Ti/Au, 50Å/800Å) was subsequently deposited on the wafer using an e-beam evaporator (Semicore Corp), followed by a lift-off process to form the interdigital transducers (IDTs).

The PDMS microchannels were fabricated using standard soft-lithography and mould-replica techniques (Fig. S1 (e–h)). The silicon substrate for the microchannel mould was patterned by photoresist (Shipley 1827, MicroChem, Newton, MA) and etched by a Deep Reactive Ion Etching (DRIE, Adixen, Hingham, MA). The silicon mould was coated with a monolayer of 1H,1H,2H,2H-perfluorooctyl-trichlorosilane

(Sigma Aldrich, St. Louis, MO) to reduce surface energy and hence the damage to the PDMS channel during the demoulding process. Sylgard^{TM} 184 Silicone Elastomer Base and Sylgard^{TM} 184 Silicone Elastomer Curing Agent (Dow Corning, Midland, MI) were mixed at an 11:1 weight ratio, cast onto the silicon mould, and cured at 70 °C for 30 min. Following that, the PDMS channel was peeled from the silicon mould, and inlets and outlets were generated on the PDMS channel using a silicon carbide drill bit.
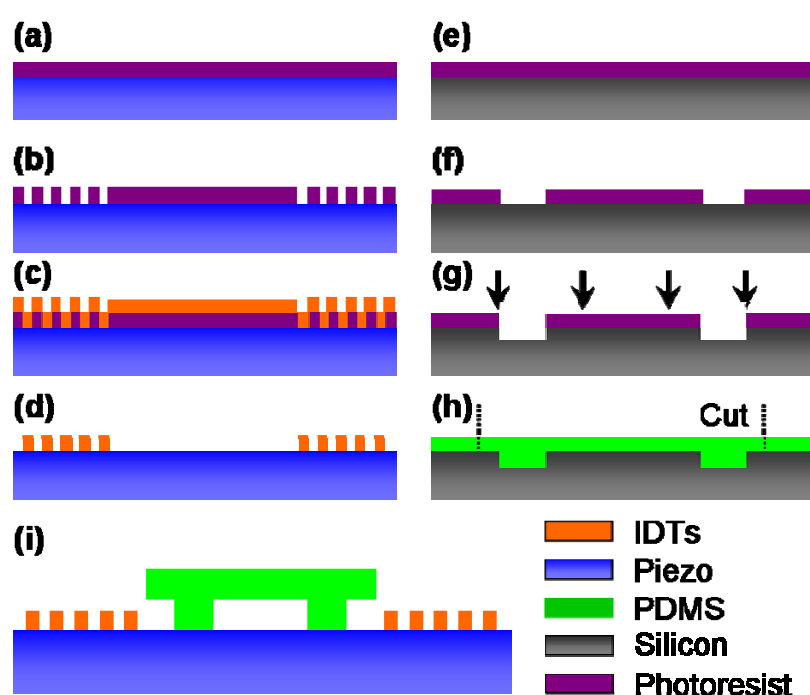
Fig. S1 Device fabrication process. (a–d) Fabrication of the SAW substrate including a metal deposition process and a following lift-off process. (e–h) A soft-lithography process was used to fabricate PDMS-based microchannels. (i) The alignment and bonding between the SAW substrate and the channel.

Lastly, oxygen plasma (50 sccm oxygen flow rate, 750 mTorr chamber pressure, and 150 W power) was utilized to activate the bonding surfaces on both the PDMS channel and the SAW device (Fig. S1i). To precisely align the channel and SAW

substrate, we fabricated alignment markers on the SAW substrate using the same process used for IDT formation and the positions of the markers corresponded to the four corners of the channel openings, which were introduced in the channel design to define the working region of SSAW. A drop of ethanol was then placed on the surface of the SAW device to serve as lubricant so that the PDMS channel could slide on top of the SAW device till the channel openings precisely overlap the alignment markers. Following that, the bonded device was left in a vacuum chamber (50 °C) to remove ethanol. Finally, polyethylene tubings (Becton Dickson, Franklin Lakes, NJ), connected to a syringe pump (KDS 210, KD scientific, Holliston, MA), were inserted into the inlet and outlet of the channel.

2. Simulation of Standing Surface Acoustic Waves

The propagation of SAW excited by IDTs on a piezoelectric substrate can be simulated by plane waves propagating with frequency-dependent attenuation. The acoustic pressure field is assumed to be uniform along the direction transverse to the wave propagation and can be expressed as

$$p(x) = p_0 \cdot e^{-\alpha x/2} \cdot e^{i(k \cdot x - 2\pi \cdot f \cdot t)}, \tag{S1}$$

where p_0, α, k, and f are the original acoustic pressure amplitude, attenuation coefficient, wave vector, and operation frequency, respectively.[S1] Using the same parameters employed in the experiments (input AC signal power P = 200 mW, SAW working area $A = 10^{-4}$ m^2), the original acoustic pressure was calculated as

$$p_0 = \sqrt{PZ/A} = 1.904e5 \,(\text{Pa}), \tag{S2}$$

where $Z = \rho \cdot c$ is the acoustic impedance, and $\rho = 4650 kg \cdot m^{-3}$, $c = 3900 m \cdot s^{-1}$ are the density and SAW velocity of the LiNbO$_3$ substrate, respectively.[S2] The frequency-dependent attenuation coefficient of SAW on this piezoelectric substrate is given by[S3]

$$\alpha = 0.19f + 0.88f^{1.9}(dB/\mu s \cdot c), \tag{S3}$$

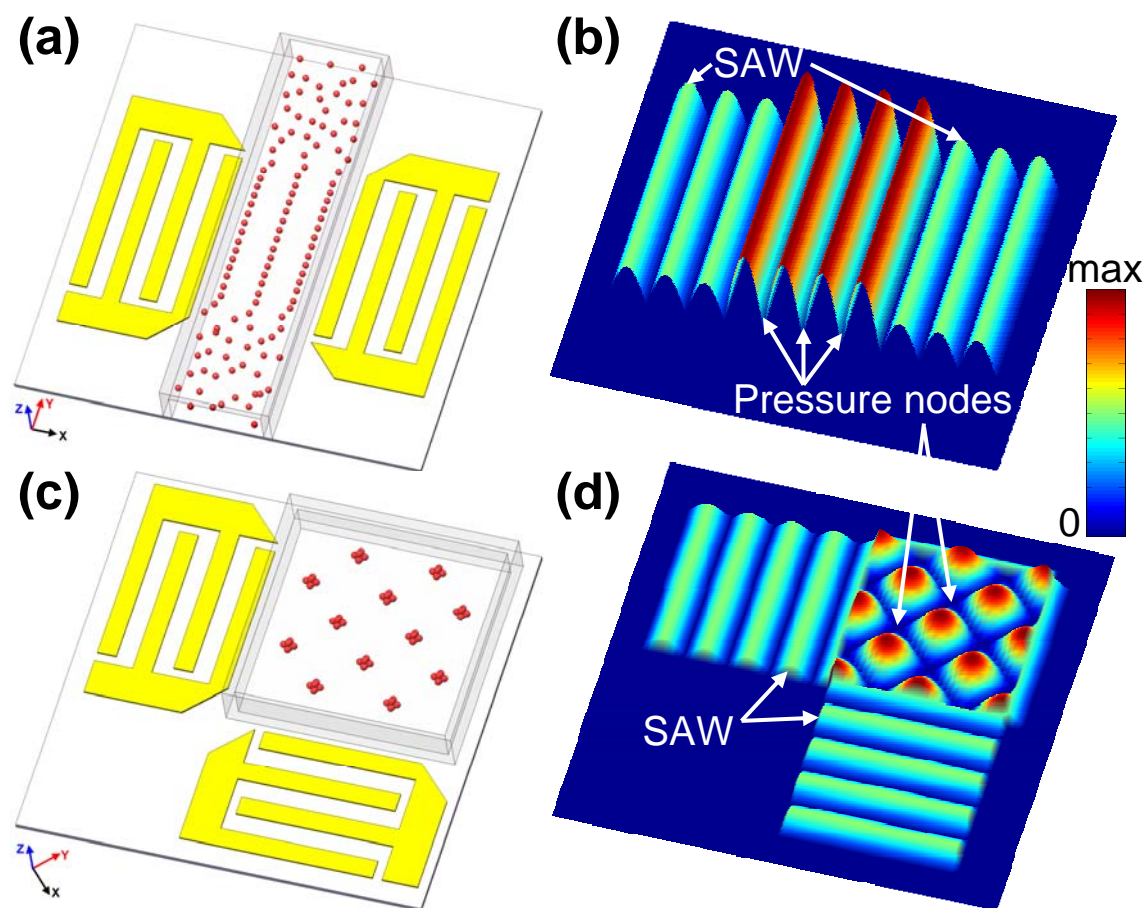where f is the SAW operation frequency (unit: GHz).

Fig. S2 Simulated pressure distribution in the SSAW field. (a) Schematic of the 1D patterning device; (b) Simulated pressure distribution based on the design in (a), showing that three pressure nodes are covered by the microfluidic channel; (c) Schematic of the 2D patterning device; (d) Simulated pressure distribution based on the design in (c), showing that pressure nodes are arranged in a square manner in the channel, resulting in 2D particle patterning.

When f =0.02 GHz, the attenuation coefficient of SAW on LiNbO$_3$ was calculated to be α =1 dB/m. Thus, the acoustic pressure field on LiNbO$_3$ could be calculated based on Eqs. S1−S3. By simulating the interference of two series of identical SAWs in opposite or orthogonal direction, we obtained the acoustic pressure

fields (Figs. S2 (b) and (d)) of the 1D and 2D SSAW-based patterning devices (Figs. S2 (a) and (c)).

Table S1 Comparison of the flow cytometry testing results for *E. coli* cells under different situations.

Sample	Total cells	Ave. FL[a]	PkPos in FL[b]	PkCnt of cell[c]
E. coli cells cultured for 12 h	20,000	0.536	0.102	6782
E. coli cells that passed through the channel without applying SSAW	20,000	0.530	0.102	6816
E. coli cells that experienced SSAW patterning	20,000	0.536	0.102	6811
E. coli cells heated at 70°C for 30 min	20,000	2.200	2.240	171

[a]Median value of the average fluorescence intensity for all cells.

[b]Peak position along fluorescence axis.

[c]Counted cell numbers at the original peak position.

3. Flow Cytometry Measurements

Freshly-prepared *E. coli* cells, grown to mid-logarithmic phase in LB media, were divided into four parts: (a) pre-treated cells cultured for 12 h (Positive Control 1), (b) cells that flow through the microchannel without applying SSAW (Positive Control 2), (c) cells that experienced the SSAW patterning process in the microfluidic system (SSAW Sample), and (d) cells that were heated at 70°C for 30 min (Negative Control). After the treatment, each group of cell culture was diluted in PBS buffer at a 1:100 ratio, and a 2 μL stock solution of $DiBAC_4(3)$ (Molecular probes, USA) was added to a

1 ml diluted cell suspension, resulting in a dye concentration of 5 μg/mL. The cells were then stained for 30 min before the flow cytometry measurement. The flow cytometry test was performed on a Beckman-Coulter XL-MCL flow cytometer using a blue-light (488 nm) excitation source. For each test, 20,000 cells were counted.

4. Thermal effect caused by SAW

The temperature of a SAW device increases during its operation due to the SAW–induced mechanical vibrations. This may potentially affect the biological objects enclosed in microchannels that are bonded with the SAW device. In order to quantify the SAW-induced thermal effect, the highest temperatures along the device under varying SAW powers were recorded by an infrared thermometer (FSI, Prism DS, Flir Instruments), and the results were plotted in Fig. S3. It is clearly shown that under the applied power used in the acoustic tweezers-based cell patterning experiments (2000 W/m^2), the device temperature is increased from 20 °C (lab temperature) to 23.5 °C. This small temperature change would generate few, if any, effects to the cells.
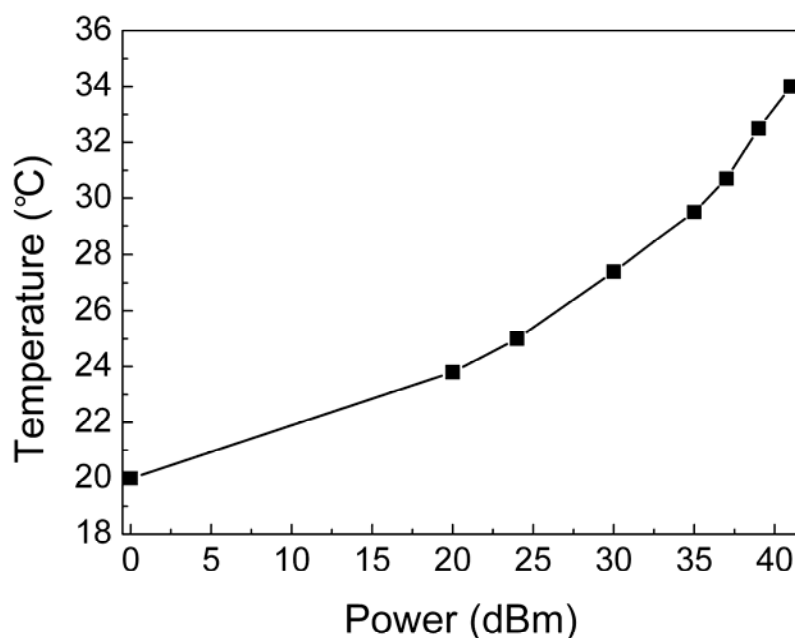
Fig. S3 Experimental data on the surface temperature under varying applied power to the SAW device (with IDT period of 100 μm, and working area 1 cm ×1 cm).

5. Quantitative Force Analysis

Based on the Stokes' law, the viscous force can be expressed as[S4]

$$F_v = 6\pi\eta r_c v_h ,$$ (S4)

where r_c, v_h, and η represent the radius of the particles, relative velocity between particles and medium, and viscosity of the surrounding medium, respectively. As r_c decreases, the viscous force F_v decreases linearly while the acoustic force F_r decreases much faster since it is proportional to r_c^3 (Fig. 4a). The calculations based on Eqs. 1, 2 and S4 reveal the dependence of acoustic and viscous forces on acoustic wavelength and particle size (Fig. 4b).

When a microparticle maintains constant velocity in the SSAW field, the acoustic and viscous forces balance each other.[S5] Based on Eqs. 1, 2 and S6, we conclude

$$v_h = -[p_0^2 V_c \beta_w /(12\lambda\eta r_c)]\phi(\rho,\beta)\sin(4\pi x/\lambda).$$ (S5)

Rewriting $v_h = -dx/dt$ and separating variables, we obtain

$$\cos ec(4\pi x/\lambda)dx = [p_0^2 V_c \beta_w /(12\lambda\eta r_c)]\phi(\rho,\beta)dt.$$ (S6)

Since the particles will move to the pressure nodes nearby, dx should be in the range of $(0, \lambda/4)$. Therefore the time needed for bead migration will be

$$t = (3\lambda^2\eta r_c /\pi)[\ln(\tan(2\pi x/\lambda))]_{x_1}^{x_2} /[p_0^2 V_c \beta_w \phi(\rho,\beta)] ,$$ (S7)

where $x_1 = 0.1(\lambda/4)$ and $x_2 = 0.9(\lambda/4)$.[S6] Figure 4d indicates that the calculated response time for the patterning processes match well with experimental results for different microparticles or cells at different wavelengths.

6. Supplemental Video

Video 1 – "1D patterning of fluorescent microparticles" (2.70 MB):

This video corresponds to the still images shown in Fig. 2c. The 1D patterning of fluorescent polystyrene beads (diameter of 1.9 μm, dragon green) via SSAW is demonstrated. The movie is in real time.

Video 2 – "2D patterning of *E. coli* cells" (2.66 MB):

This video corresponds to the still images shown in Fig. 3b of the article. The 2D patterning of *E. coli* cells (processed with fluorescent dye) via SSAW is demonstrated. The time scale has been compressed by a factor of 2.

References:

S1. A.D. Pierce. *Acoustics-An Introduction to Its Physical Principles and Applications*, Acoustical Society of America, NY, 1989.

S2. K.K. Wong. *Properties of Lithium Niobate*, INSPEC, London, 2002.

S3. D. Supriyo. *Surface acoustic wave devices*, Englewood Cliffs, NJ: Prentice-Hall, 1986.

S4. G. K. Batchelor. *An Introduction to Fluid Dynamics*, Cambridge University Press, Cambridge, England, 1967.

S5. R. K. Gould and W. T. Coakley, The effects of acoustic forces on small particles in suspension.*In proceedings of the 1973 symposium on Finite Amplitude Wave Effects in Fluids*, Copenhague, DANEMARK, 1974, pp. 252–257.

S6. L. Toft and A. D. D. Mckay. *Practical Mathematics*, Pitman Publishing Corporation, London, 1946.